Available online at www.sciencedirect.com
ScienceDirect
Icarus 184 (2006) 29–38
ICARUS
www.elsevier.com/locate/icarus

Atlas of the mean motion resonances in the Solar System

Tabaré Gallardo *

Departamento de Astronomia, Facultad de Ciencias, Igua 4225, 11400 Montevideo, Uruguay

Received 30 December 2005; revised 29 March 2006

Available online 19 May 2006

Abstract

The aim of this work is to present a systematic survey of the strength of the mean motion resonances (MMRs) in the Solar System. We know by applying simple formulas where the resonances with the planets are located but there is no indication of the strength that these resonances have. We propose a numerical method for the calculation of this strength and we present an atlas of the MMRs constructed with this method. We found there exist several resonances unexpectedly strong and we look and find in the small bodies population several bodies captured in these resonances. In particular in the inner Solar System we find one asteroid in the resonance 6:5 with Venus, five asteroids in resonance 1:2 with Venus, three asteroids in resonance 1:2 with Earth and six asteroids in resonance 2:5 with Earth. We find some new possible co-orbitals of Earth, Mars, Saturn, Uranus and Neptune. We also present a discussion about the behavior of the resonant disturbing function and where the stable equilibrium points can be found at low and high inclination resonant orbits.

Keywords: Celestial mechanics; Resonances; Trans-neptunian objects; Near-Earth objects; Trojan asteroids

1. Introduction

For many years the dynamical studies of MMRs were restricted to low order resonances because these are the most evident in the asteroid belt. High order resonances, however, started to appear in studies of highly eccentric orbits like those of comets (Chambers, 1997), NEAs (Morbidelli and Nesvorný, 1999), trans-neptunians (Robutel and Laskar, 2001) and specially meteors streams (Emel'yanenko, 1992), becoming the capture in high order MMR a not so uncommon phenomena. It is laborious to identify which one of the hundreds of MMRs that theoretically exist near the semimajor axis of the orbit we are studying is the one affecting the body's motion. This difficulty is due to the absence of a simple method that adequately weighs the strength of each resonance. Neither we have a global view of the strength of the resonances with all the planets over all Solar System. Authors have opted to plot the resonance's strength as a function that decreases as resonance's order increases (Nesvorný and Morbidelli, 1998), but this criteria gives equal strength for all resonances of the same order which is unrealistic. For zero inclination orbits it is possible to compute the widths in semimajor axis of the MMRs with the planets as a function of the eccentricity (Dermott and Murray, 1983; Morbidelli et al., 1995; Nesvorný et al., 2002) but no simple method exists to compute the widths in the case of non-zero inclination orbits. We present here a method to estimate the strength of the mean motion resonant orbits with arbitrary orbital elements. The method is a modification and an extension of the author's method recently proposed (Gallardo, 2006). Based on this principle we compute the strength of the resonances with all the planets form Mercury to Neptune for all ranges of semimajor axis, from the Sun up to 300 AU assuming typical orbital eccentricities and inclinations of populations of small bodies like near-Earth asteroids (NEAs), centaurs, trans-neptunian objects (TNOs) and scattered disk objects (SDOs).

This work is organized as follows. In Section 2 we show how to evaluate numerically the disturbing function $R(\sigma)$ for a resonant orbit. In Section 3 we analyze the possible shapes of $R(\sigma)$ and the location of the equilibrium points defined by its minima. In Section 4 we define the strength function $SR(e, i, \omega)$ for a given resonance and we analyze its shape. In Section 5 we calculate SR for thousands of resonances with all the planets except Pluto, we analyze the generated atlas and look for real

* Fax: +598 2 5250580.
E-mail address: gallardo@fisica.edu.uy.

0019-1035/$ – see front matter
doi:10.1016/j.icarus.2006.04.001

objects showing the predicted behavior. In Section 6 we present the conclusions.

2. Numerical evaluation of the resonant disturbing function

Given a planet of mass m_P and radius vector $\mathbf{r}_P$ in an heliocentric frame and a small body at $\mathbf{r}$ the disturbing function is:

$$\mathbb{R} = k^2 m_P \left(\frac{1}{|\mathbf{r}_P - \mathbf{r}|} - \frac{\mathbf{r}\cdot\mathbf{r}_P}{r_P^3} \right). \tag{1}$$

Since Laplace's times astronomers looked for an analytical expression for $\mathbb{R}$ as an explicit function of the orbital elements. We will refer the reader to Gallardo (2006), for example, for a detailed explanation of the general form of the disturbing function. In this paper we will assume circular and zero inclination orbits for the planets designed here by the subscript P. Under this hypothesis and taking into account D'Alembert rules a q-order resonance $|p+q| : |p|$ with p and q integers occurs when the general critical angle

$$\sigma_j = (p+q)\lambda_P - p\lambda - (q-2j)\varpi - 2j\Omega = \sigma + 2j\omega \tag{2}$$

librates or have a slow time evolution, where

$$\sigma = (p+q)\lambda_P - p\lambda - q\varpi \tag{3}$$

is the principal critical angle and j is an integer positive or negative. Due to the long period of the angles (ϖ, Ω) the librations of σ_j occur approximately for

$$\frac{n}{n_P} \simeq \frac{p+q}{p}, \tag{4}$$

where the n's are the mean motions. Then, the formula

$$\frac{a}{a_P} \simeq (1+m_P)^{-1/3} \left(\frac{p}{p+q} \right)^{2/3} \tag{5}$$

defines the location of the resonances in semimajor axis. At very low eccentricities the time variation of ϖ cannot be ignored and the location of the resonances are shifted respect to Eq. (5). The integer p is the degree of the resonance with $p<0$ for exterior resonances and $p>0$ for interior resonances. With this notation the trojans (or co-orbitals) correspond to $p=-1$ and $q=0$. The resonant motion is generated when there is a strong dependence of $\mathbb{R}$ on σ which must be librating or in slow time-evolution. In this case $\mathbb{R}(\sigma)$ dominate the time evolution of the orbital elements.

For a specific resonance defined by a semimajor axis given by Eq. (5) we eliminate all short period terms on $\mathbb{R}$ computing the mean disturbing function

$$R(\sigma) = \frac{1}{2\pi|p|} \int_0^{2\pi|p|} \mathbb{R}\big(\lambda_P, \lambda(\lambda_P,\sigma)\big)\, \mathrm{d}\lambda_P \tag{6}$$

for a given set of fixed values of $(e, i, \varpi, \Omega, \sigma)$, where we have expressed $\lambda = \lambda(\lambda_P, \sigma)$ from Eq. (3) with σ as a fixed parameter and where $\mathbb{R}(\lambda_P, \lambda)$ is evaluated numerically from (1), where $\mathbf{r}_P$ and $\mathbf{r}$ were expressed as functions of the orbital elements and mean longitudes λ_P and λ. This numerical mean disturbing function is valid for a particle that strictly satisfies the condition $\sigma = constant$ but we will consider it representative also for a real object showing a slow evolution during the period of time in which the integral (6) is calculated, that means $|p|$-times the planet's orbital period. We repeat for a series of values of σ between $(0°, 360°)$ obtaining a numerical representation of the resonant disturbing function $R(\sigma)$.

If the particle's orbit intersects the planet's orbit for a certain value of σ the integral (6) diverges due to divergence of Eq. (1). We are not interested in calculating $R(\sigma)$ in that circumstance for that specific value of σ because we know the resonant motion is impossible due to the collision with planet. Then, in the implementation of the numerical calculation of the integral (6) by a simple equally spaced abscissa method we discard the points where $\mathbb{R}$ from Eq. (1) diverges.

According to theoretical series expansions, at low eccentricity and low inclination orbits $R(\sigma)$ should follow a sinusoid with amplitude proportional to e^q. But the shape of $R(\sigma)$ for high eccentricities or high inclinations cannot be defined from classical analytical expansions because they are not valid in that circumstances.

3. The shape of $R(\sigma)$ and the libration centers

The equations of the resonant motion show that the time evolution of the semimajor axis, $\mathrm{d}a/\mathrm{d}t$, is proportional to $\partial R/\partial\sigma$ then the shape of $R(\sigma)$ is crucial because it defines the location of stable and unstable equilibrium points. For specific values of (e, i, ω) the minima of $R(\sigma)$ define the stable equilibrium points also known as *libration centers* around which there exist the librations. The unstable equilibrium points are defined by the maxima.

We found that at low (e, i) the function $R(\sigma)$ calculated from Eq. (6) is very close to a sinusoid as one can expect from the classical series expansions (see low left panels of Figs. 1, 2 and 4). At higher e the orbit approaches to the planet's orbit, $R(\sigma)$ start to depart from the sinusoid and classical series expansions start to fail with some exceptions like Beauge's expansion valid for the planar case (Beaugé, 1996). For eccentricities greater than the collision eccentricity e_c:

$$e_c \simeq \left| 1 - \left(\frac{p+q}{p} \right)^{2/3} \right| \tag{7}$$

the orbit can intersect the planet's orbit and for low inclination orbits two peaks start to appear around the point where $R(\sigma)$ has its maximum for $e < e_c$. If the two peaks can be distinguished then a stable equilibrium point appears between them. For high inclination orbits the intersection between orbits is less probable and soft maxima can appear instead of the peaks. As $R(\sigma)$ is 2π-periodic in σ there is always at least one minimum which corresponds to a stable equilibrium point. For small inclination orbits the libration centers are almost independent of (i, ω) but for high inclination orbits the libration centers strongly depend on (i, ω) and due to the time evolution of ω the libration centers evolve as ω evolves in long timescales.

The sharp peaks that can appear for orbits with $e > e_c$ in all the resonant disturbing functions are produced by close encounters between planet and particle. Low inclination orbits with a small minimum orbit intersection distances (MOID) with respect to the planet's orbit will show two peaks. For high inclination orbits the MOID is in general greater than for low inclination orbits and also dependent on ω so the peaks will be less pronounced and strongly dependent on ω. This strongly modifies the shape of $R(\sigma)$ and consequently the location of the equilibrium points. In fact for low eccentricity and high inclination orbits the equilibrium points could be better defined by angles like $\sigma_j = \sigma + 2j\omega$ from Eq. (2) instead of σ (see Fig. 6 of Gallardo, 2006).

Looking at the shape of $R(\sigma)$ all resonances can be classified in only three different classes as we explain below.

3.1. General behavior of $R(\sigma)$ for 1:n resonances including trojans

Resonances of the type 1:n including trojans (that means 1:1) exhibit a similar general behavior showed in Fig. 1. For $e < e_a$ where $e_a < e_c$ there is a libration center at $\sigma = 180°$ and for $e > e_a$ there appear the asymmetric libration centers (Beaugé, 1994) with locations depending not only on e but also on (i, ω). For trojans we have $e_a = e_c = 0$ so the low eccentricity librations around $\sigma = 180°$ do not exist. For $e > e_a$ horseshoe (HS) trajectories wrapping the asymmetric librations can exist. These HS trajectories are of the same nature of the horseshoe trajectories in the case of trojans and are only possible for this kind of resonances. In HS trajectories σ is oscillating with high amplitude around 180°. For $e > e_c$ at low inclinations they appear two peaks (unstable equilibrium points) and a stable libration center at $\sigma = 0°$. This last equilibrium point is associated with the known quasi-satellites (QS) of the 1:1 resonances (Wiegert et al., 2000). In Section 5 and Tables 1 and 2 we present some small bodies that are QS of a planet or will be temporarily captured as QS.

3.2. General behavior of $R(\sigma)$ for odd order interior resonances

For low inclination orbits all odd order interior resonances show librations around $\sigma = 0°$, and for $e > e_c$ it appears another libration point at $\sigma = 180°$ (Fig. 2). For high inclination orbits the geometry of the encounters is strongly modified which affects the peaks of $R(\sigma)$ and its shape becomes completely different to the planar case. As in the case of resonances of type 1:n the libration centers become strongly dependent on ω. For example, in Fig. 2 it appears a libration center at $\sigma \sim 70°$ which we have verified by a numerical integration and we show in Fig. 3.

3.3. General behavior of $R(\sigma)$ for all other resonances

For low inclination orbits all interior resonances of order even and all exterior resonances except resonances of type 1:n show librations around $\sigma = 180°$, and for $e > e_c$ it appears another libration point at $\sigma = 0°$ (Fig. 4). Again, for high inclinavion orbits the geometry of the encounters is strongly modified and the shape of $R(\sigma)$ becomes strongly dependent on ω.

It is necessary to stress that $R(\sigma)$ as showed in Figs. 1, 2 and 4 describes the resonant disturbing function, but a particular resonant orbit will not strictly follow $R(\sigma)$ because the resonant motion involves small oscillations of e, i and specially a. These oscillations produce some departures of $R(\sigma)$ with respect to

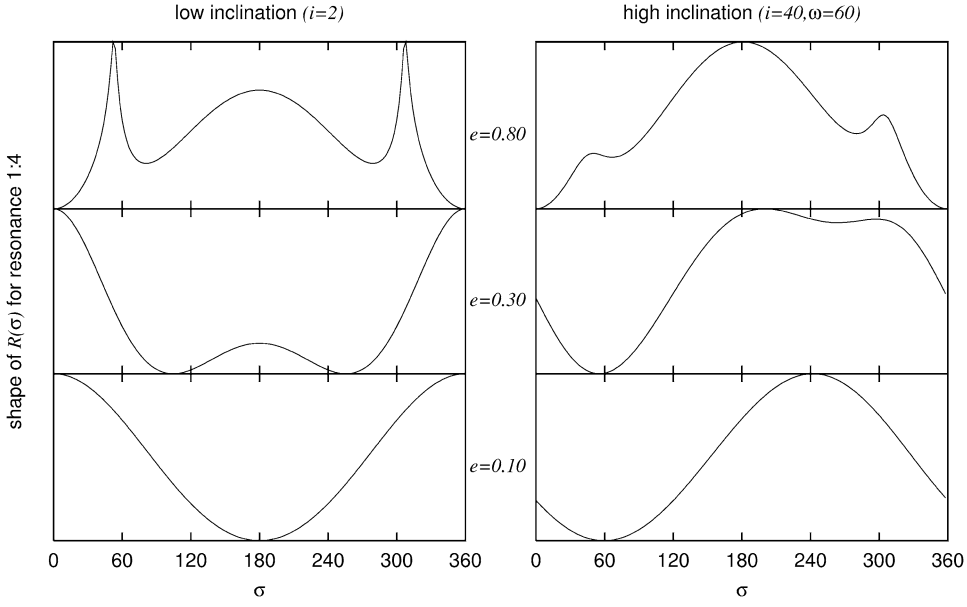

Fig. 1. General behavior of $R(\sigma)$ for 1:n resonances for three values of e and two values of i. The lower plot correspond to $e < e_a < e_c$ (see text), at left three plots for low inclination orbits and at right for high inclination orbits. Trojans also exhibit this behavior except the lower panel because for trojans $e_c = e_a = 0$. Stable librations are possible at minima of $R(\sigma)$ but the asymmetric librations also allow HS trajectories wrapping both asymmetric libration islands, so σ seems to oscillate around 180° with very high amplitude. For high inclination orbits the shape of $R(\sigma)$ is completely distorted and shallow minima can appear besides of a well defined one.

Table 1
Some real asteroids in unusual mean motion resonances

Designation	a (AU)	e	i (°)	ω (°)	Resonance	σ (°)
2004 XY60	0.640	0.79	23.7	131	6:5V*	Lib. at 320, amp. 150
2002 VE68	0.723	0.41	8.9	356	1:1V	QS
2001 CK32	0.725	0.38	8.1	234	1:1V	HS
2004 GU9	1.000	0.13	13.6	281	1:1E	QS
1994 TF2	0.993	0.28	23.7	350	1:1E	HS-QS
2004 BO41	0.997	0.47	34.9	256	1:1E*	HS-QS-L
(85770) 1998 UP1	0.998	0.34	33.1	234	1:1E*	HS-QS-L
2001 GO2	1.006	0.16	4.6	265	1:1E	HS-QS
2000 WN10	1.001	0.29	21.4	225	1:1E*	HS-QS-L
2002 AA29	0.994	0.01	10.7	100	1:1E	HS
2003 YN107	0.997	0.01	4.2	84	1:1E	HS
(3753) Cruithne	0.997	0.51	19.8	44	1:1E	HS
1997 AQ18	1.147	0.46	17.3	37	1:2V*	Lib. at 290, amp. 40
2000 EF104	1.147	0.41	10.8	347	1:2V*	Lib. at 295, amp. 15
2005 ML13	1.147	0.24	6.8	221	1:2V*	Lib. at 80, amp. 40
2002 AA	1.147	0.30	11.2	65	1:2V*	HS
1994 CB	1.149	0.14	18.2	288	1:2V	HS
2001 DH47	1.522	0.03	24.3	16	1:1M	Lib. at 290, amp. 40
(5261) Eureka	1.523	0.06	20.2	96	1:1M	Lib. at 301, amp. 6
(101429) 1998 VF31	1.524	0.10	31.2	310	1:1M	Lib. at 295, amp. 25
1999 UJ7	1.524	0.03	16.7	48	1:1M	Lib. at 70, amp. 40
(36017) 1999 ND43	1.522	0.31	5.5	52	1:1M*	HS
2005 XD1	1.586	0.29	17.9	199	1:2E*	HS
1996 DH	1.586	0.27	17.2	351	1:2E*	Lib. at 280, amp. 40
2000 VF39	1.587	0.16	33.7	221	1:2E*	Lib. at 70, amp. 40
2000 SC45	1.841	0.17	25.3	77	2:5E*	Lib. at 165, amp. 115
2004 JY6	1.841	0.07	32.8	348	2:5E*	Lib. at 180, amp. 60
2004 XB	1.841	0.09	11.7	61	2:5E*	Lib. at 130, amp. 50
2004 RQ9	1.842	0.09	18.4	85	2:5E*	Lib. at 320, amp. 30
1999 JB11	1.842	0.25	37.1	31	2:5E*	Lib. at 170, amp. 170
2003 YP22	1.842	0.11	16.3	267	2:5E*	Lib. at 230, amp. 120

Last column indicates the approximate libration center and amplitude deduced form numerical integrations including all the planets. The critical angle σ is defined as in Eq. (3). Quasi satellites are noted as QS, horseshoes as HS and temporary captures in a Lagrangian point as L. The location of the libration centers can be understood analyzing the shape of $R(\sigma)$ as explained in Section 3. An * means original results.

Table 2
Same as Table 1 for some real centaurs, TNOs and SDOs in unusual mean motion resonances in the outer Solar System

Designation	a (AU)	e	i (°)	ω (°)	Resonance	σ (°)
2005 NP82	5.875	0.47	130.5	254	5:6J*	Lib. at 330, amp. 60
(15504) 1999 RG33	9.378	0.77	34.9	274	1:1S*	Temporary QS
2003 LH7	15.39	0.20	22.9	359	1:2S 1:5J*	HS
(83982) 2002 GO9	19.53	0.28	12.7	93	1:1U*	HS
2000 SN331	19.60	0.04	11.5	346	1:1U*	QS-HS
2002 CA249	22.01	0.43	6.3	203	2:7S*	Lib. at 200, amp. 150
2002 DH5	22.17	0.36	22.4	328	2:7S*	Lib. at 180, amp. 60
2000 CO104	24.23	0.14	3.0	139	1:4S*	Lib. at 120, amp. 100
(55576) 2002 GB10	25.26	0.39	13.3	239	2:3U*	Lib. at 180, amp. 130
2005 TO74	30.12	0.01	5.2	18	1:1N	Lib. at 65, amp. 30
2001 XA255	30.12	0.68	12.6	89	1:1N 1:2U*	Transition
2005 TN53	30.13	0.00	24.8	333	1:1N	Lib. at 65, amp. 25
2001 QR322	30.13	0.02	1.3	153	1:1N	Lib. at 65, amp. 30
2004 UP10	30.17	0.06	1.4	42	1:1N	Lib. at 70, amp. 30
2002 GB32	218.4	0.83	14.1	37	1:18N*	Libration and HS
(82158) 2001 FP185	227.2	0.84	30.7	7	1:19N*	Libration and HS
2000 CR105	222.52	0.80	22.7	317	4:79N*	Lib. at 180, amp. 90

Quasi satellites are noted as QS and horseshoes as HS. An * means original results.

the figures obtained from Eq. (6) but not substantial modifications occur in its shape. Also, in case of orbits with very small MOID and in consequence with a sharp peak in $R(\sigma)$ for a certain σ_{peak} a real object certainly will not evolve following $R(\sigma)$ when $\sigma = \sigma_{\text{peak}}$ because the strong perturbation by the planet will broke the resonant motion.

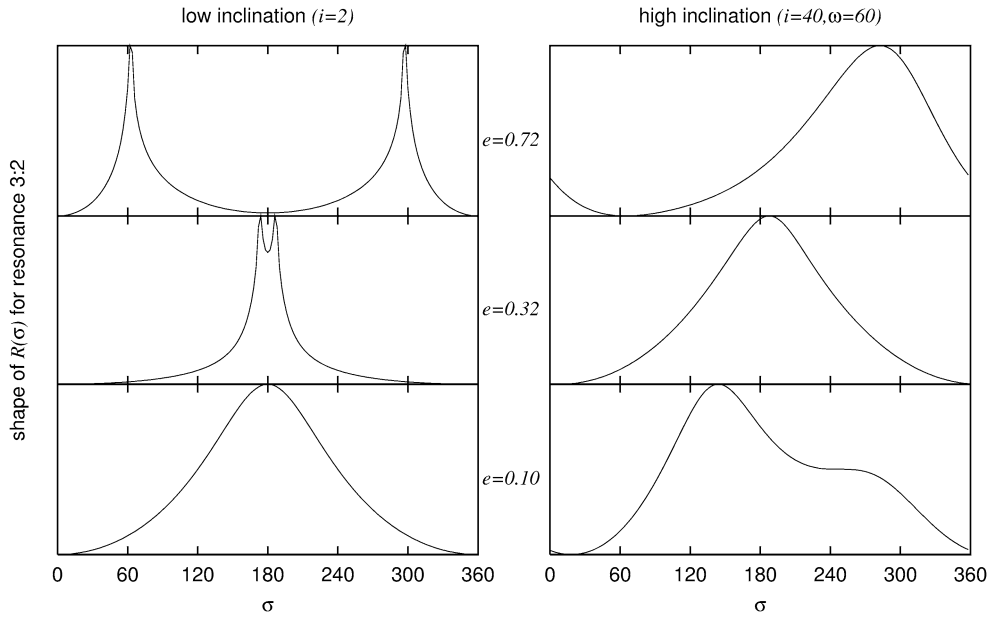

Fig. 2. General behavior of $R(\sigma)$ for all odd order interior resonances for three values of e and two values of i. The lower plot corresponds to $e < e_c$. See Fig. 4 for comparison. In analogy to Fig. 1, for high inclination orbits the shape of $R(\sigma)$ is completely distorted. The equilibrium point that appears in the top right plot at $\sigma \sim 70°$ is verified in Fig. 3.

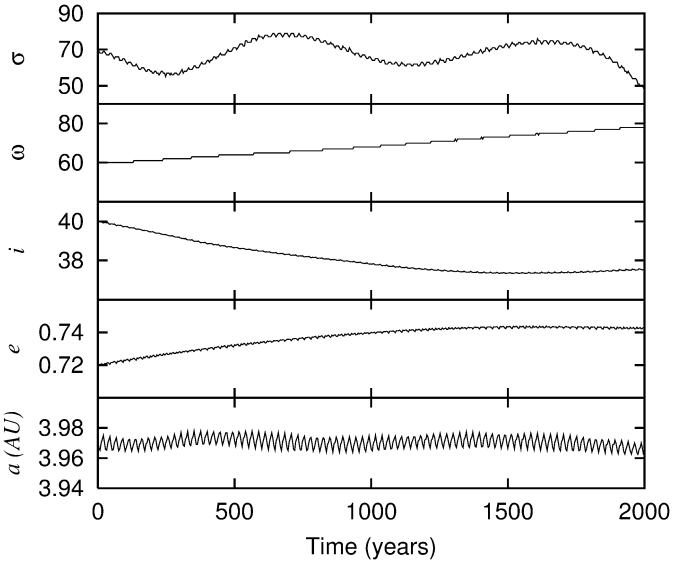

Fig. 3. Verification of the existence of the stable equilibrium point at $\sigma \sim 70°$ deduced from Fig. 2. Numerical integration of an hypothetical particle at resonance 3:2 with Jupiter. The libration center is strongly linked to (i, ω). The libration period (poorly distinguished in a) is approximately 800 years.

4. Numerical estimation of the resonance's strength $SR(e, i, \omega)$

For a given resonant orbit defined by parameters $(a, e, i, \varpi, \Omega)$ the disturbing function $R(\sigma)$ is determined. We define the strength function SR as:

$$SR(a, e, i, \omega) = \langle R \rangle - R_{\min} \tag{8}$$

being $\langle R \rangle$ the mean value of $R(\sigma)$ with respect to σ and $R_{\min}$ the minimum value of $R(\sigma)$. This definition is in agreement with the coefficients of the resonant terms of the expansion of the disturbing function for low (e, i) orbits because for this case $R(\sigma)$ is a sinusoid with an amplitude given by $\langle R \rangle - R_{\min}$. This definition of strength function is not substantially distorted by the peaks that $R(\sigma)$ can show for orbits with very small MOID so we can also use it for these cases. A definition of SR based on $R_{\max} - R_{\min}$, for example, will be more affected by the peaks $R_{\max}$.

We recall that in the resonant motion $\mathrm{d}a/\mathrm{d}t \propto \partial R/\partial\sigma$. If $SR \sim 0$ we have $\partial R/\partial\sigma \sim 0$ for all values of σ and then $\mathrm{d}a/\mathrm{d}t$ will not be dominated by resonant terms but by other terms that will generate some time evolution of the semimajor axis and consequently the resonance will be broken, so the resonance will not be dynamically significant or strong. On the contrary, a high value of SR implies a strong dependence of R on σ and the resonant disturbing function $R(\sigma)$ will dominate the motion forcing the semimajor axis to evolve oscillating around the stable equilibrium points or to evolve escaping from the unstable equilibrium points.

We analyzed the shape of $SR(e, i, \omega)$ for several resonances and we found that all them can be roughly classified in two classes ($q \leqslant 1$ and $q \geqslant 2$) that we present below. In the plots and calculus we present in this work we will take the unit of mass such that $k^2 m_{\mathrm{Jupiter}} = 1$, being k the Gaussian constant of gravitation.

The first class of resonances is composed by trojans and all first order interior and exterior resonances. They show a somehow similar global behavior of $SR(e, i, \omega)$ regarding high inclination and low inclination orbits (Fig. 5). For low inclination orbits the strength is in general something greater than for high inclination orbits. Precise values of SR depends on the resonance and also on ω but the general view is not substantially modified.

On the other hand, all interior and exterior resonances with order $q \geqslant 2$ show a similar global behavior of $SR(e, i, \omega)$ re-

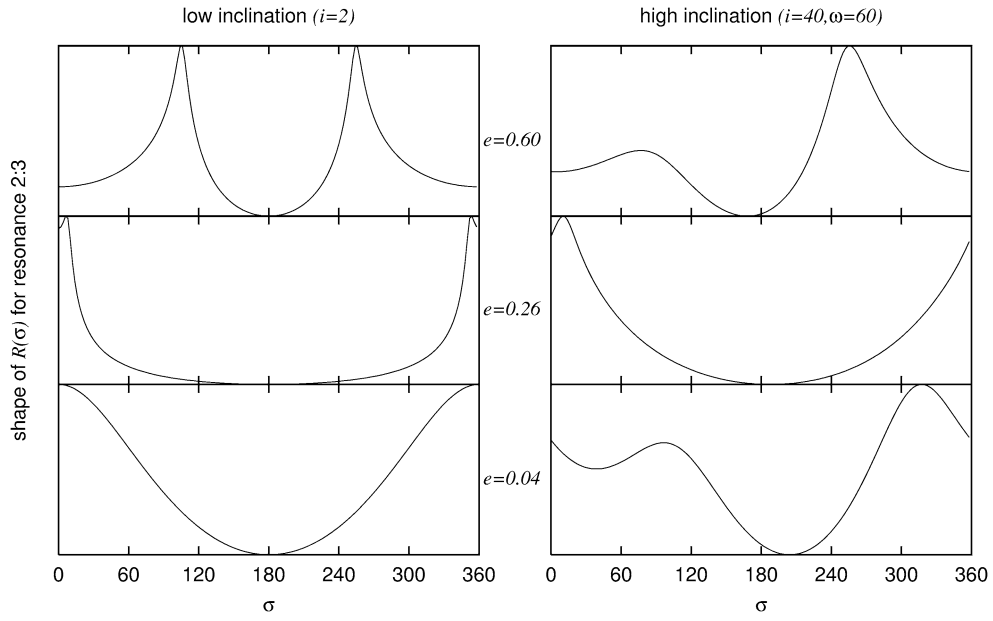

Fig. 4. General behavior of $R(\sigma)$ for three values of e and two values of i for even order interior resonances and all exterior resonances except 1:n. The lower plot corresponds to $e < e_c$. Compare this figure with Fig. 2.

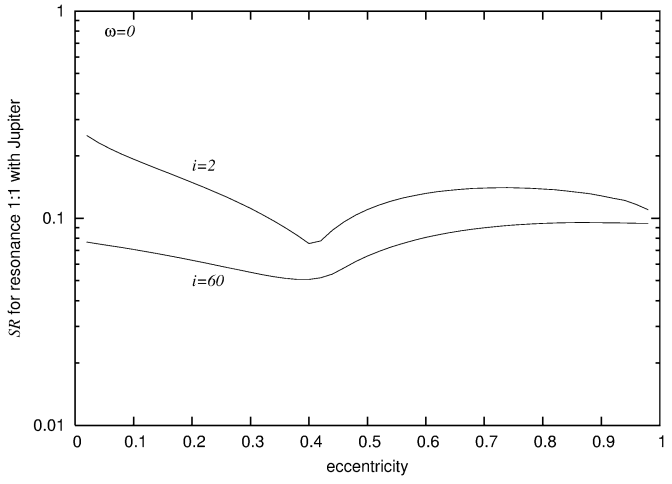

Fig. 5. Typical behavior of the strength function *SR* for trojans and all first order resonances ($q \leqslant 1$). Low inclination orbits are in general something stronger than high inclination orbits. This particular plot corresponds to Jupiter's trojans but all first order resonances show a similar behavior with respect to the inclination.

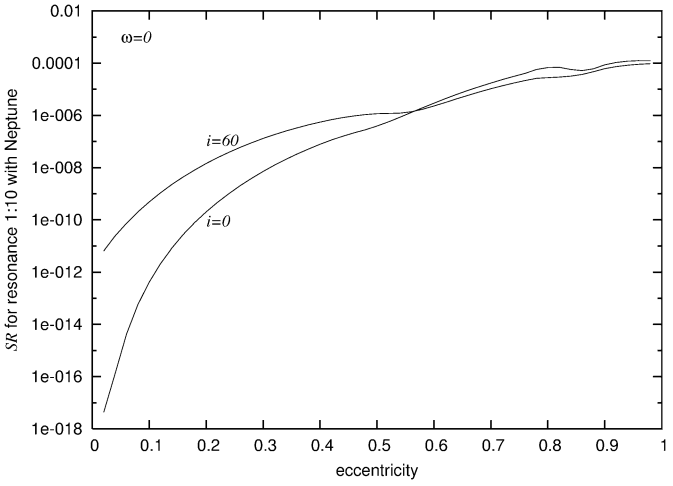

Fig. 6. Typical strength for all interior and exterior resonances of order $q \geqslant 2$. At low eccentricities the resonances are stronger for high inclination orbits and at high eccentricities the inclination do not affect substantially the resonance's strength. This particular plot corresponds to resonance 1:10 with Neptune.

garding high inclination and low inclination orbits (Fig. 6). For low eccentricity orbits the strength can be several orders of magnitude greater for high inclination orbits than for low inclination orbits. This is in good agreement with Robutel and Laskar (2001) where is it found that at low eccentricities the resonances are more evident for high inclination orbits. For high eccentricity orbits both high and low inclination resonant orbits have comparable *SR*. The limit between low and high eccentricities depends on each resonance.

It is possible to understand why the inclination is an important factor for resonances of order 2 or greater. Analytical developments of $R(\sigma)$ in powers of (e, i) show that for a q-order resonance the lowest order resonant terms are of order q in (e, i) (Murray and Dermott, 1999). In particular for trojans (Morais, 1999) and first order resonances the lowest order terms are independent of i. But, for resonances of order $q \geqslant 2$ the lowest order resonant terms have a dependence with i that make some contribution to $R(\sigma)$ for high inclination orbits (Gallardo, 2006). These analytical developments are valid for relatively small eccentricities. In consequence is natural that for resonances of order 2 or greater at low eccentricity regime the resonances are stronger for high inclination orbits because the resonant terms depending on i will show up. On the contrary we cannot expect such behavior for resonances of order 1 or 0 because the resonant terms depending on i have lower relevance.

5. Atlas of MMRs and examples

For a given resonance with a given planet its strength *SR* is a function of (e, i, ω) as we have explained in the previous section. Then, a specific small body will experience the effects of the resonances according to its orbital elements. We take typical orbital elements (e, i) for different populations and calculate the strength of all resonances verifying $|p + q| < 100$ and order $q < 100$ with all the planets from Mercury to Neptune. In the region between 0 and 6 AU we used typical orbital elements of NEAs ($e = 0.46, i = 15°$). For the centaurs' region between 6 to 25 AU we assumed typical centaurs' orbital elements ($e = 0.46, i = 32°$). For the region between 25 and 48 AU we used typical TNOs' orbital elements ($e = 0.2, i = 10°$). For the scattered disk region between 48 and 300 AU we assumed a population with perihelion distances of 32 AU and $i = 20°$. We assume always an arbitrary $\omega = 60°$. By this way we construct an atlas of resonance's strengths presented in Fig. 7 which can be considered representative for the populations above mentioned.

We have also numerically integrated the full equations of motions for small bodies at low ($a < 2$ AU) and high ($a > 5.8$ AU) semimajor axis and looked for resonant motions. We found several objects evolving in somehow unusual resonances an some of them are identified in a resonant motion by first time. The most interesting results are presented in Tables 1 and 2. The orbital elements were taken from ASTORB (ftp://ftp.lowell.edu/pub/elgb/astorb.html) by December 2005 and the integrator used was EVORB (www.fisica.edu.uy/~gallardo/evorb.html) including the planets from Mercury to Neptune. Some small bodies have important uncertainties in their orbital elements, specially the new objects and the SDOs, so the real dynamics is not exactly as we have found in our numerical integrations. But the fact that we have found they evolve driven by unusual mean motion resonances demonstrates the importance of these resonances usually not considered in dynamical studies of minor bodies.

5.1. NEA-type orbits between the terrestrial planets

Low order resonances with Venus and Earth dominate the region from 0 to 1.5 AU and resonances like 1:2E, 2:5E and 3:8E are strong and relatively isolated in the region between 1.5 to 2.0 AU (Fig. 7a), so objects could survive in these resonances if encounters with Mars can be avoided. In Table 1 we present several real objects that we have found at some of these resonances. Some of these objects were already identified in resonant motions (Christou, 2000; Brasser et al., 2004) and others are now identified as resonant objects for first time. Both hypothetical Venus' and Earth's trojans are relatively isolated from other strong resonances but Mars' and Mercury's trojans should be strongly perturbed by other resonances of comparable strength. The values (e, i) we have adopted is something exaggerated for real trojans. For lower values of (e, i) the trojans approximately maintain the strength (see Fig. 5) while the strength for the other resonances fall so low eccentricity trojans can survive better and this is exactly that we see for Mars' trojans (Table 1).

According to its present orbital elements the asteroid 2004 XY60 is being captured in 6:5V with a libration center at $\sigma \sim 320°$ which is the precise value where the corresponding $R(\sigma)$ have its minimum. It is known that 2002 VE68 is a QS of Venus (Mikkola et al., 2004) and in our integrations 2004 GU9 is a QS of the Earth at present and for approximately 500 years in the future.

In Table 1 we present five objects evolving in 1:2V despite their semimajor axis being very near Earth's semimajor axis, one of them already identified in this resonance by Bykova and Galushina (2001). In particular 2000 EF104 is evolving in the deep resonance with a very low amplitude libration. We have found the new candidate (36017) 1999 ND43 in 1:1M with high eccentricity in a HS trajectory. We present for first time three objects at 1:2E, very near Mars' orbit and six objects at 2:5E. In particular, objects 1995 DH and 2000 VF39 show a very stable evolution in the deep resonance 1:2E.

Two of the six objects evolving in the resonance 2:5E, 2004 XB and 2004 RQ9, seem to have a very stable evolution with very low amplitude librations of the critical angle. See in Table 1 that for this last resonance the libration centers are not always located at $\sigma = 180°$ as we could deduce for a low inclination theory and, as we have explained in Section 3, the libration centers depends also on (i, ω). However, objects 2004 RQ9 and 2003 YP22 have their libration centers at a different position than predicted by our model due to secular terms generated by the planets that our resonant model does not contemplate.

5.2. High eccentricity orbits in the region of asteroids and Jupiter

The region between 2 and 2.5 AU is full of resonances with Venus, Earth and Mars with comparable strength (Fig. 7b). These kind of resonances are also present between 2.5 and 3 AU but this region up to 6 AU is completely dominated by MMRs with Jupiter (Fig. 7c). Ours Figs. 7b–7c can be compared with Fig. 2 from Nesvorný et al. (2002) where widths of main resonances with Mars, Jupiter and Saturn are showed for zero inclination orbits. Our results are in agreement with that results for resonances with Jupiter and Saturn. Results for resonances with Mars are difficult to compare. Resonances with Mars were identified as a source of chaos in the inner asteroid belt (Morbidelli and Nesvorný, 1999), but according to our results resonances with Venus, Earth and Mars have comparable strengths at high eccentricity regime. Looking at our Fig. 7a and taking into account we have found some objects in resonance with Venus and Earth we can conclude that also in the region $2 < a < 2.5$ AU resonances with Venus and Earth should be considered in the dynamical studies.

Very close to 2:1J is 5:1S but it is two to three orders of magnitude weaker and analogously Jupiter's trojans have very near the weak 5:2S. Resonances 2:1, 7:4, 5:3, 3:2, 7:5, 4:3 and 5:6 with Jupiter are strong and clearly isolated from others (Figs. 7b–7c). We found that according to the nominal orbit from ASTORB the exotic object 2005 NP82 is captured in 5:6J (Table 2). This is a retrograde object in highly eccentric orbit

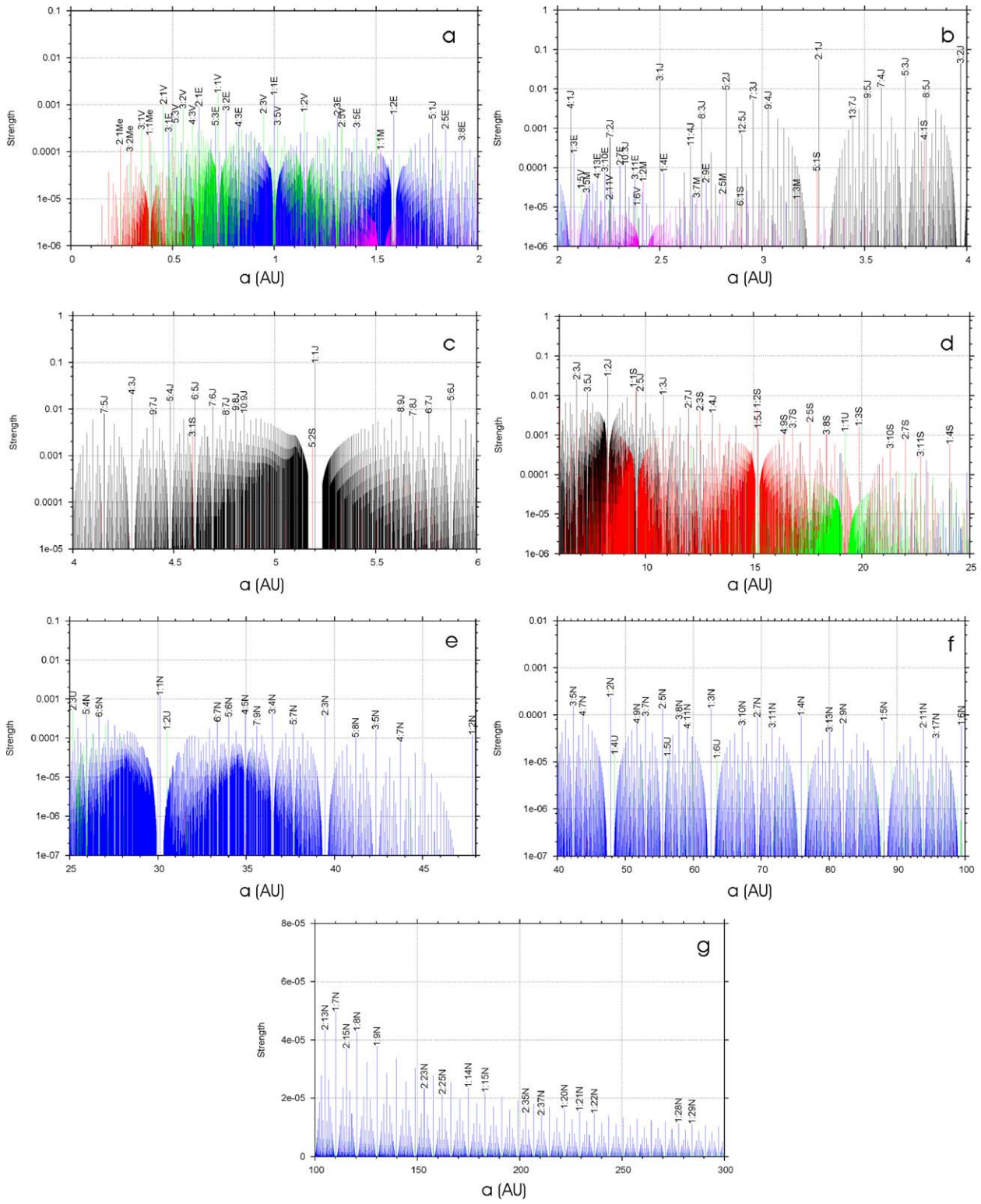

Fig. 7. Atlas of MMRs in the Solar System verifying $|p+q|<100$ and with order $q<100$ calculated for different set of values $(e, i, \omega = 60^\circ)$ characteristic of some populations of minor bodies. (a) Terrestrial planets' region. The resonance's strength is calculated for typical NEAs' orbits ($e = 0.46, i = 15^\circ$). Resonances with Venus and Earth dominate. Between 1.5 and 2 AU resonances 1:2E, 2:5E and 3:8E are strong and isolated. (b) Asteroids' region. The resonance's strength is calculated as in (a). Between 2 and 2.5 AU several high order resonances with Venus, Earth and Mars compete with resonances due to Jupiter. Note the behavior of the strength of the family of resonances near 2:1J slightly perturbed by 5:1S and the isolation of resonance 3:2J. (c) Jupiter's region. The resonance's strength is calculated as in (a). The pattern is due to Jupiter which dominate this region. Jupiter's trojans are perturbed by 5:2S. (d) Centaurs' region. The resonance's strength is calculated for orbits with $e = 0.46, i = 32^\circ$. Note the superposition of resonances with Jupiter and Saturn. (e) Neptune's and TNOs' region. The resonance's strength is calculated for orbits with $e = 0.2, i = 10^\circ$. The pattern of the resonances in this region is imposed by Neptune. Neptune's trojans could be affected by 1:2U. (f) Scattered disk objects' region. The resonance's strength is calculated for SDOs evolving with $q = 32$ AU and assuming $i = 20^\circ$. (g) The farthest regions of the Solar System. The resonance's strength is calculated as in (f). In this plot the scale in strength is linear. Resonances 1:n with Neptune dominate.

which is librating around $\sigma \sim 330°$ exactly as our model predicts for the location of the minimum of $R(\sigma)$. We have not analyzed the real population inside Jupiter's orbit because there is an extended literature about that (see Nesvorný et al., 2002, for a review).

5.3. Centaurs' domains

Most important exterior resonances with Jupiter are affected by resonances with Saturn and conversely Saturn's trojans, for example, are strongly affected by 2:5J (Fig. 7d). Due to the quasi commensurability between Jupiter and Saturn, in the region between 6 and 16 AU it does not exist a strong and isolated MMR. However in the region from 16 to 20 AU some resonances with Saturn like 3:7 and 2:5 could dominate if encounters with Uranus are avoided. Uranus' trojans are affected by high order resonances with Saturn. The object 2003 LH7 with $a \simeq 15.4$ AU is in a well defined HS trajectory inside the 1:2S resonance and simultaneously shows a HS trajectory inside the resonance 1:5J although not so well defined as the former.

We found a very eccentric ($e \simeq 0.77$) co-orbital of Saturn in HS trajectory with transitions to QS ((15504) 1999 RG33). Objects 2002 GO9 and 2000 SN331 are co-orbitals of Uranus in HS trajectories having the last one a temporary evolution as QS in the future (Table 2). Near Uranus' orbit we found 2 objects in 2:7S and one object (2000 CO104) in 1:4S.

5.4. Neptune's and TNOs' region

The region between 25 and 30 AU is full of MMR with Uranus and Neptune (Fig. 7e). Between 34 and 48 AU there are several strong and isolated MMR with Neptune like 3:4, 2:3, 3:5, 4:7 and specially 1:2 that we do not study here because they were well analyzed by several authors (see, for example, Nesvorný and Roig, 2001).

The object (55576) 2002 GB10 being in 2:3U is a kind of "plutino" of Uranus showing high amplitude librations but very stable evolution during the 10,000 years of our numerical integration. According to Fig. 7e, Neptune's trojans appear isolated and objects in 1:2U could exist if they can avoid close encounters with Neptune. We identified five objects in 1:1N, one of them (2001 XA255) showing a chaotic evolution with transition from 1:1N to 1:2U (Table 2).

5.5. The region of the scattered disk

Following results from Fernandez et al. (2004), to evaluate the resonance's strength in this region we assume a population of SDOs diffusing outwards to the Oort cloud with perihelion distance $q = 32$ AU and with $i = 20°$. Resonances of the type 1:n are not only the strongest but also they have no strong resonances in their proximities, so they should dominate over other resonances (Figs. 7f–7g). Nevertheless, resonances of the type 2:n are also relatively strong and isolated. Resonances 1:n with Uranus are near some resonances with Neptune but probably safely shifted in semimajor axis (Fig. 7f). Our figures can be compared with the ones by D. Nesvorný that can be found at www.boulder.swri.edu/~davidn/kbmmr and where it is possible to see that resonances of type 1:n with Neptune clearly dominate and are isolated from other resonances.

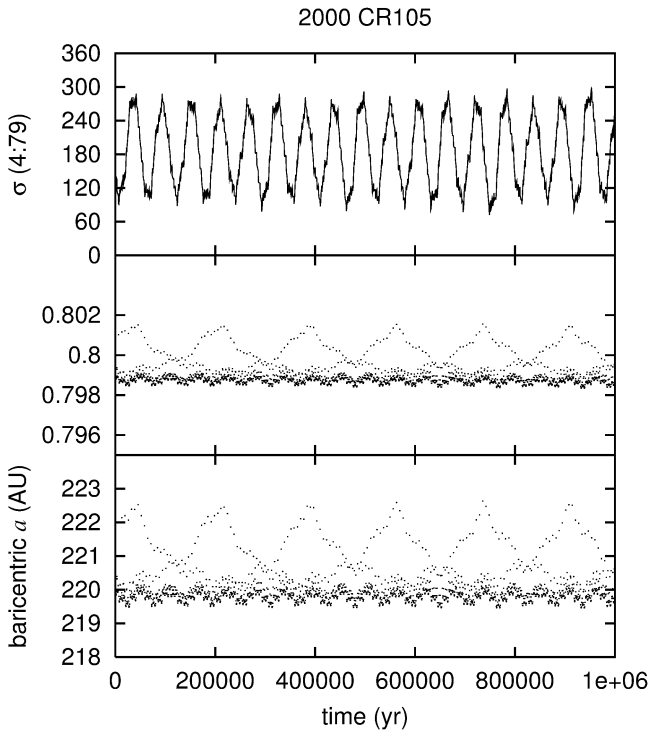

Fig. 8. Resonant motion of 2000 CR105 inside the resonance 4:79N according to nominal orbit from ASTORB. The critical angle is $\sigma = -4\lambda_N + 79\lambda - 75\varpi$.

We have integrated by 1 Myr the orbits of the farthest objects in the scattered disk taking into account the planets from Jupiter to Pluto. Objects 2002 GB32 and (82158) 2001 FP185 were identified at 1:18N and 1:19N, respectively, showing transitions between asymmetric librations and HS trajectories (Table 2). Nevertheless, the uncertainties in the semimajor axis of 2002 GB32 are so high (around 3 AU) that we cannot asseverate the real object is captured in the resonance. The object 2000 CR105, that has been analyzed by several authors (Gladman et al., 2002; Morbidelli and Levison, 2004; Gomes et al., 2005; Gallardo, 2006) deserves some comments. According to our very short numerical integration using the nominal orbit from ASTORB this object is locked in the very high order resonance 4:79N (Fig. 8). Taking into account the uncertainties in its semimajor axis, it is more reasonable that analogously to 2002 GB32 and (82158) 2001 FP185 it had been captured in a resonance of the type 1:n, in particular 1:20. The fact that the critical angle of the resonance 4:79 is librating is not a proof that the real orbit of 2000 CR105 is in that resonance but is a confirmation that very high order resonances are relevant at very high eccentricities.

Finally, it is important to stress that the strengths presented in Fig. 7 were obtained for specific values of (e, i, ω). Using different values of these orbital elements will produce different strengths but the general view will be roughly maintained. The most important parameter is the eccentricity; for lower eccentricities the high order resonances will drop respect to the low

order ones, and for higher eccentricities all resonances tend to comparable values.

6. Conclusions

According to the shape of the resonant disturbing function $R(\sigma)$ all resonances can be classified in three different groups: (a) type 1:n, (b) odd order interior resonances and (c) even order interior resonances and all exterior resonances excluding the 1:n resonances. Horseshoe trajectories wrapping two libration centers are only possible for the first class. For high inclination orbits the shape of $R(\sigma)$ is generally very different from the low inclination case and it becomes strongly dependent on ω. For high inclination orbits $R(\sigma)$ loses its symmetry with respect to $\sigma = 0°$ and $\sigma = 180°$ and the stability and locations of libration centers is modified.

We have defined the resonance's strength SR as a function that measures the amplitude of the changes in the resonant disturbing function $R(\sigma)$ due to the critical angle σ. According to the behavior of the strength SR as a function of (e, i) it is possible to distinguish 2 groups of resonances: (1) those with $q \leqslant 1$ always something stronger for low inclination orbits and (2) those with $q \geqslant 2$. At low eccentricities, the second group of resonances is stronger for high inclination orbits than for low inclination orbits. The different behavior of these two groups can be understood considering the terms of the classical expansion of the resonant disturbing function that depend on the orbital inclination. These terms are relevant for resonances of order $q \geqslant 2$ and not relevant for resonances of order $q \leqslant 1$.

Using our method we have identified several strong and isolated resonances along the Solar System. The method, for example, provides realistic evaluation of the strength of the families of resonances like $(n + 1)$:n and n:$(n + 1)$ that are present at both sides of 1:1 resonance. All them are of order 1 so they would be equally weighted using a simple criteria based only on the order.

According to our plots in the region $1 < a < 2.5$ AU resonances with Venus, Earth and Mars are at least as strong as resonances with Jupiter. This was confirmed finding some real objects evolving in that resonances. Some real objects were identified experiencing unusual resonances like 6:5V, 1:2V, 1:2E, 2:5E, 5:6J, 1:2S, 1:5J, 2:7S, 1:4S, 2:3U, 1:2U, 1:18N, 1:19N and 4:79N, some of them in very stable orbits.

According to our results there should be some interaction between resonances with Jupiter and Saturn. For example, 2:1J and 1:1J should be slightly perturbed by 5:1S and 5:2S, respectively, and 1:1S and 1:2S strongly perturbed by 2:5J and 1:5J, respectively. It is possible that in some circumstances objects in 1:1N could be perturbed by 1:2U as is showed by the object 2001 XA255 in our numerical integrations.

At very high eccentricities like the ones we can found in the SDOs population very high order resonances with Neptune are strong enough to show up and probably dominate the dynamical evolution.

Tables with strengths calculated for thousands of resonances and fortran codes for calculate $R(\sigma)$ and $SR(e, i, \omega)$ can be obtained requesting to the author.

Acknowledgments

The author acknowledges the criticism given by D. Nesvorný and another anonymous referee. This work was developed in the framework of the "Proyecto CSIC I + D, Dinamica Secular de Sistemas Planetarios y Cuerpos Menores."

References

Beaugé, C., 1994. Asymmetric librations in exterior resonances. Celest. Mech. Dynam. Astron. 60, 225–248.

Beaugé, C., 1996. On a global expansion of the disturbing function in the planar elliptic restricted three-body problem. Celest. Mech. Dynam. Astron. 64, 313–350.

Brasser, R., Innanen, K.A., Connors, M., Veillet, C., Wiegert, P., Mikkola, S., Chodas, P.W., 2004. Transient co-orbital asteroids. Icarus 171, 102–109.

Bykova, L.E., Galushina, T.Yu., 2001. Evolution of near-Earth asteroids close to mean motion resonances. Planet. Space Sci. 49, 811–815.

Chambers, J.E., 1997. Why Halley-types resonate but long-period comets don't: A dynamical distinction between short and long-period comets. Icarus 125, 32–38.

Christou, A.A., 2000. A numerical survey of transient co-orbitals of the terrestrial planets. Icarus 144, 1–20.

Dermott, S.F., Murray, C.D., 1983. Nature of the Kirkwood gaps in the asteroid belt. Nature 301, 201–205.

Emel'yanenko, V.V., 1992. Dynamics of periodic comets and meteors streams. Celest. Mech. Dynam. Astron. 54, 91–110.

Fernandez, J.A., Gallardo, T., Brunini, A., 2004. The scattered disk population as a source of Oort cloud comets: Evaluation of its current and past role in populating the Oort cloud. Icarus 172, 372–381.

Gallardo, T., 2006. The occurrence of high order mean motion resonances and Kozai mechanism in the scattered disk. Icarus 181, 205–217.

Gladman, B., Holman, M., Grav, T., Kavelaars, J., Nicholson, P., Aksnes, K., Petit, J.-M., 2002. Evidence for an extended scattered disk. Icarus 157, 269–279.

Gomes, R.S., Gallardo, T., Fernandez, J.A., Brunini, A., 2005. On the origin of the high-perihelion scattered disk: The role of the Kozai mechanism and mean motion resonances. Celest. Mech. Dynam. Astron. 91, 109–129.

Mikkola, S., Brasser, R., Wiegert, P., Innanen, K., 2004. Asteroid 2002 VE68, a quasi-satellite of Venus. Mon. Not. R. Astron. Soc. 351, L63–L65.

Morais, M.H.M., 1999. A secular theory for Trojan-type motion. Astron. Astrophys. 350, 318–326.

Morbidelli, A., Levison, H.F., 2004. Scenarios for the origin of the orbits of the trans-neptunian objects 2000 CR105 and 2003 VB12 (Sedna). Astron. J. 128, 2564–2576.

Morbidelli, A., Nesvorný, D., 1999. Numerous weak resonances drive asteroids toward terrestrial planets orbits. Icarus 139, 295–308.

Morbidelli, A., Thomas, F., Moons, M., 1995. The resonant structure of the Kuiper belt and the dynamics of the first five trans-neptunian objects. Icarus 118, 322–340.

Murray, C.D., Dermott, S.F., 1999. Solar System Dynamics. Cambridge Univ. Press, Cambridge, UK.

Nesvorný, D., Morbidelli, A., 1998. Three-body mean motion resonances and the chaotic structure of the asteroid belt. Astron. J. 116, 3029–3037.

Nesvorný, D., Roig, F., 2001. Mean motion resonances in the trans-neptunian region. Icarus 150, 104–123.

Nesvorný, D., Ferraz-Mello, S., Holman, M., Morbidelli, A., 2002. Regular and chaotic dynamics in the mean-motion resonances: Implications for the structure and evolution of the asteroid belt. In: Bottke, W.F., Paolicchi, P., Binzel, R.P., Cellino, A. (Eds.), Asteroids III. Univ. of Arizona Press, Tucson, pp. 379–394.

Robutel, P., Laskar, J., 2001. Frequency map and global dynamics in the Solar System I. Icarus 152, 4–28.

Wiegert, P., Innanen, K., Mikkola, S., 2000. The stability of quasi-satellites in the outer Solar System. Astron. J. 119, 1978–1984.